Peer-reviewed version available at *Materials* **2018**, *11*, 2379; doi:10.3390/ma11122379

Article

Drilling of γ-TiAl intermetallic alloys. Mechanistic model to predict cutting force and torque

Aitor Beranoagirre [1,*], Gorka Urbikain [1], Amaia Calleja [2] and L. N. López de Lacalle [3]

[1] Department of Mechanical Engineering, University of the Basque Country (UPV/EHU), Plaza Europa 1, 20018 San Sebastián, Spain; gorka.urbikain@ehu.eus
[2] Department of Mechanical Engineering, University of the Basque Country (UPV/EHU), Nieves Cano 12, 01006 Vitoria, Spain; amaia.calleja@ehu.eus
[3] CFAA, University of the Basque Country (UPV/EHU), Parque Tecnológico de Zamudio 202, 48170 Bilbao, Spain; norberto.lzlacalle@ehu.es
* Correspondence: aitor.beranoagirre@ehu.eus; Tel.: +34-943-018-636

Abstract: Gamma titanium aluminides (γ-TiAl) present an excellent behaviour under high temperature conditions, being a feasible alternative to nickel-based superalloy components in aeroengine sector. However, considered as a difficult to cut material, process cutting parameters require special study to guarantee components quality. In this work, developed drilling mechanistic model is a useful tool in order to predict drilling force (F_z) and torque (T_c) for optimal drilling conditions determination. The model is validated for three types of Gamma-TiAl alloys. Integral hard metal end-drilling tools and different cutting parameters (feeds and cutting speeds) are tested in three different sized holes for each alloy.

Keywords: Gamma-TiAl, superalloys, slight materials, drilling, titanium aluminides.

1. Introduction

Aeronautic is an emerging sector, aircraft manufacturing predictions estimate to double current fleet by the year 2033, in order to satisfy passenger's increment demand that grows at a rate of 4.2% per year [1]. Components manufacturing for the aeronautic sector is a high value added process, and, concretely, motor components require special attention because they represent one of the most expensive (20%) components [2]. Aviation industry will try to satisfy manufacturing demand according to regulations requirements regarding efficiency, noise, fuel consumption and contamination. Therefore, new materials and manufacturing processes are under development by aeronautic sector manufacturers. In this sense, γ-TiAl alloys are a feasible replacement for nickel-based alloys frequently used for compressor blades and stator in gas turbine aeroengines [3-5]. Moreover, titanium alloys are also interesting for bio-medical engineering, automobile sector and chemical industries [6].

Gamma titanium aluminide intermetallics present excellent strength-weight ratio, and corrosion resistance at high temperature [7]. However, it is considered a difficult to cut material [8, 9] due to its poor tensile and low room temperature ductility (<2%). Besides, high heat values are generated during γ-TiAl machining due to material low thermal conductivity. Consequently, tool and workpiece wear mechanism are accelerated [10], tool life is reduced and workpiece integrity is affected. Moreover, γ-TiAl reacts chemically with many materials causing material adhesion.

Peer-reviewed version available at Materials 2018, 11, 2379; doi:10.3390/ma11122379

Several studies have considered γ-TiAl a difficult to cut material regarding turning [11, 12], grinding [13], high speed milling [14-16], drilling and micro-drilling [17].
In this sense, high machining conditions can cause irreversible consequences such as surface cracking, hardened layers and tensile residual stresses [18]. Optimal machining strategies and parameters are studied for electrochemical machining [19], turning [20, 21], and milling [22] related to cutting temperature techniques evaluation, and, appropriate machining conditions determination in order to reduce tool wear and increase tool life. Milling studies have also investigated the effects of operating parameters and conditions on tool life and surface integrity when milling γ-TiAl alloys [23-25].

In relation to lubrication techniques, some studies [26] focus on cryogenic lubrication (liquid nitrogen) obtaining cutting feed values increment while tool life is maintained.
Machining processes modelling is also a well-known field for difficult to cut materials. In this sense, two-dimensional models [27] are developed for cutting parameters such as cutting speed and feed influence determination. Empirical models are also used for thrust and torque values prediction in composites. Other techniques such as response surface methodology (RSM) and finite element analysis (FEA) are implemented for milling [28] and drilling [29] process parameters analysis. In addition finite element models are also developed for performance characteristics such as hole quality prediction [30].

Considering γ-TiAl promising application possibilities, drilling machinability studies are a focus of interest due to presented machinability problems being drilling one of the most frequent processes for components assembling. In this work, developed drilling mechanistic model is a useful tool in order to predict drilling force (F_z) and torque (T_c) for optimal drilling conditions determination. The model is validated for three types of Gamma-TiAl alloys. Integral hard metal end-drilling tools and different cutting parameters (feeds and cutting speeds) are tested in three different sized holes for each alloy.

2. Experimental procedure

2.1. Material

Four different titanium alloys are tested in performed drilling tests: Ti-6Al-4V and three different γ-TiAl alloys (TNB, extruded MoCuSi and ingot MoCuSi). Table 1 shows tested alloys mechanical properties.

γ-TiAl alloys present higher aluminum percentage in comparison to other titanium such as Ti-6Al-4V, 43-48% in γ-TiAl and 6% in Ti-6Al-4V, improving thermal conductivity in γ-TiAl. On the other hand, ductile transition temperature occurring between 600-800ºC, depending on the microstructure and grain size alloys, is aggravated for alloys with higher titanium percentage [11]. The intermetallic TiAl provides low density [31] as well as high mechanical strength under high temperatures and corrosive environments. The intermetallic γ-TiAl superalloys offer excellent mechanical properties [32], with low density (4gr/cm3), high resistance at high temperatures, low electrical and thermal conductivity, oxidation resistance, ultimate strength of 1000 MPa and Young's modulus of 160 GPa.

MoCuSi alloy [Ti-(43-46) Al-(1-2) Mo-(0.2) Si-Cu] is used at low temperatures with high resistance below 650ºC, and, TNB alloy [Ti-(44-45) Al-(5-10)Nb-(0.2-0.4)C] resists very high temperatures maintaining high resistance and oxidation values. Regarding MoCuSi alloys, the material is presented in both, extruded o ingot structure. Extruded alloys present an oriented structure oriented in the extrusion direction whereas melted alloys present a structure without any preferable orientation, typical of no extruded or laminated materials. The ingot structure is directly obtained from VAR (Vacuum Arc Remelting) process. For extruded structures, material is extruded at 1200ºC and smaller sized grains are obtained with superior creep strain, yield strength and KIC.

Peer-reviewed version available at Materials 2018, 11, 2379; doi:10.3390/ma11122379

Table 1. Mechanical properties comparison between TiAl alloys.

PROPERTY	TNB	Ti–6Al–4V (annealed)	MoCuSi extruded	MoCuSi ingot
Density (g/cm³)	3.86	4.49	3.74	3.88
Specific modulus (GPa/Mg/m³)	43	24	43	37
Tensile strength (MPa)	683	1087	607	689
Specific strength (MPa/g/cm³)	192	947	198	180
Yield strength (MPa)	589	942	589	570
Ductility (%)	1.9	7.8	1.7	2.4
Fracture toughness (MPa m$^{1/2}$)	23	52	23	20
Thermal conductivity (W/mK)	24	8.6	24	19
Maximum operating temperature (ºC)	900	615	900	865

2.2. *Equipment*

Machining tests were performed in a vertical CNC milling machine, Kondia® model B640, with maximum rotational speed of 10,000 rpm and 25 kW. During the tests, process-cutting conditions are measured and recorded. For the axial/thrust (F_z) and radial (F_x, F_y) cutting forces, and, Z axis (T_c) torque measurements, a dynamometric Kistler® equipment 9257B was used.

Figure 1. Kondia® model B640 (left) and Kistler® 9257B dynamometer (right)

2.3. *Machining conditions*

Drilling tests were carried out for the described four titanium alloys (Table 1). As it can be seen in Table 2, for each material, tested feed values are 0.05 and 0.1 mm/rev, and, D = 3-5-7 and 8.5 mm holes were drilled in each case. The drilled depth is 20 mm.

Table 2. Machining conditions for the 8.5 mm hole

Material	V_c [m/min]	N [rev/min]	f [mm/rev]	f [mm/rev]
Ti-6Al-4V	50	1874	0.05	0.1
TNB	15	1874	0.05	0.1
MoCuSi Extruded	15	562	0.05	0.1
MoCuSi Ingot	15	562	0.05	0.1

Preprints (www.preprints.org) | NOT PEER-REVIEWED | Posted: 29 October 2018 doi:10.20944/preprints201810.0646.v1

Peer-reviewed version available at Materials 2018, 11, 2379; doi:10.3390/ma11122379

The selected tool is a solid carbide drill (Mitsubishi®, MPS0850S-DIN-C, Figure 2). During the machining operations cutting forces, torque and power consumption were recorded.

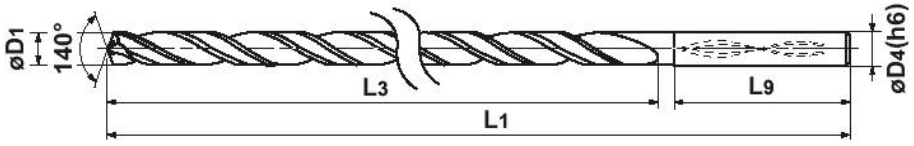

Figure 2. Cutting tool geometry

One of the critical aspects when drilling γ-TiAl is chip evacuation and heat dissipation. Internal lubrication is directly applied on the cutting edge, due to the poor thermal conductivity of these alloys. Specially designed for low machinability materials, Rhenus® FU W (Table 3) coolant was used. Internal coolant pressure is set to 8.5 bar.

Table 3. Properties of Rhenus FU 70 W coolant

CONCENTRATED		EMULSION	
Viscosity 20 ºC (mm²/s)	Content of mineral oil %	pH Value 5% concentration	Protection against corrosion (DIN 51360/1)
Approx. 150	Approx. 33	Approx. 9,0	Note 0 al 2%

3. Cutting forces prediction mechanistic model

Predictive cutting forces mechanistic models help programmers with cutting parameters selection. Especially when drilling low machinability titanium alloys, it is interesting to simulate different machining conditions in order to decide whether the estimated cutting forces values led to an optimum machining process

This section explains the modelling of cutting forces and torque in drilling. Since the cutting speed varies along the drill's lips, the way the cutting force coefficients are introduced inside the model is a crucial issue. There have been a number of attempts based on orthogonal-oblique transformation [33] and mechanistic models [34].

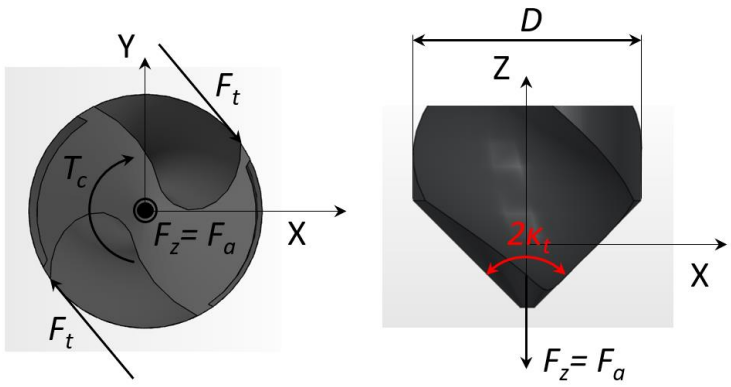

Figure 3. Cutting or tangential force (F_t), thrust force (F_z) and cutting torque (T_c) in drilling process. Drill bottom view (left) and front view (right).

The cutting edge is divided into discrete elements in the drill axis (j=1 to n elements) and the global cutting force and torque are obtained by summing the elemental contributions along each lip (i=1 to Z). As it can be seen in Figure 3, while F_x and F_y are coupled due to tool rotation leading to the

radial Fr and tangential Ft cutting force components, F_z is directly obtained from the axial component Fa. Here, we will focus on the thrust force (Eq.1) in Z direction and torque (Eq.2), which are critical parameters when characterizing tool life. These magnitudes are calculated as:

$$F_z(t) = \sum_{i=1}^{Z}\sum_{j=1}^{n} K_{c,z}(h,r)\cdot \Delta z \cdot h \quad (1)$$

$$T_c(t) = \sum_{i=1}^{Z}\sum_{j=1}^{n} K_{t,z}(h,r)\cdot \Delta z \cdot h \cdot r \quad (2)$$

where K_z and K_T are the corresponding thrust force and torque coefficients, Δz is the axial width of a differential element and h the chip thickness (here, $h = 0.5f{\cdot}sin70°$). As usual, the thrust cutting force and torque coefficients need to be calibrated. Here, 4 different titanium alloys were tested: 1) Ti-6Al-4V, taken as reference; 2) TNB and MoCuSi types, 3) extruded and 4) ingot types. Under this approach the cutting force coefficients were assumed as function of feedrate (or h) and radial distance of the cutting point to drill axis as quadratic functions. First, a_0-a_5 and b_0-b_5 coefficients in Eqs. (3-4) are identified from a linear regression for the four types of materials from a set of experiments.

$$K_z(h,r) = a_0 + a_1\cdot h + a_2\cdot r + a_3\cdot hr + a_4\cdot r^2 + a_5\cdot h^2 \quad (3)$$

$$K_T(h,r) = b_0 + b_1\cdot h + b_2\cdot r + b_3\cdot hr + b_4\cdot r^2 + b_5\cdot h^2 \quad (4)$$

4. Results

The mechanistic model is valid for V_c = 50 m/min (Ti-6Al-4V), and V_c = 15 m/min (TNB, and extruded/ingot types), the cutting speed at the tool diameter D. To identify the cutting coefficients 10 tests were done. After a pilot hole the hole was finished at D = 8.5 mm. Five different pilot hole diameters (D_0 = 3-4-5-6-7 mm) and two feed rates (f = 0.05-0.1 mm) were programmed.

Results for Ti-6Al-4V alloy

As it can be seen, both experimental and the predicted thrust force and torque values are higher for higher feed rate values (Figure 4). Table 4 shows the experimental data for both variables during the calibration of the cutting coefficients. While the curve F_z reflects almost a linear tendency, the torque is approximated as a curve with an inflexion (third order). At the same time, the higher dispersion is found the lower is the difference between the pilot and final hole diameters.

Table 4. Experimental results for F_z [N] and T_c [Nm] in Ti-6Al-4V alloy.

	F_z [N]		T_c [Nm]	
D_0 [mm]	f [mm/rev]		f [mm/rev]	
	0.05	0.1	0.05	0.1
3	591	723	3.1	3.9
4	460	565	2.4	3.7
5	319	440	2.1	3.4
6	242	332	1.9	3.2
7	169	225	1.8	3.1

Preprints (www.preprints.org) | NOT PEER-REVIEWED | Posted: 29 October 2018 doi:10.20944/preprints201810.0646.v1

Peer-reviewed version available at Materials 2018, 11, 2379; doi:10.3390/ma11122379

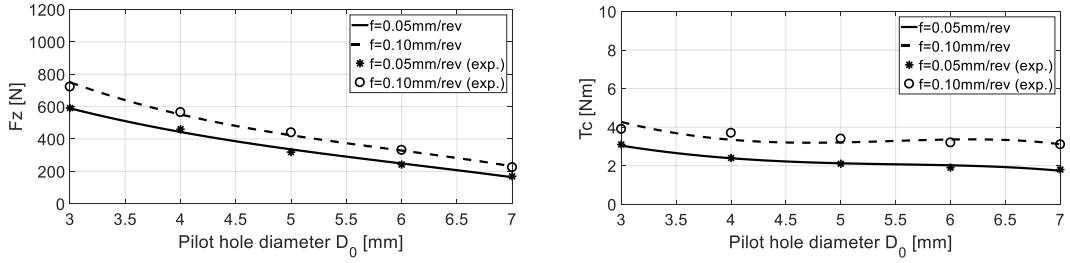

Figure 4. F_z [N] (left) and T_c [Nm] (right) for Ti-6Al-4V alloy drilling experimental and mechanistic model values

Results for TNB alloy

Thrust force values (Figure 5 left) show higher values for higher feed rate values but are not doubled when doubling the feed rate. However, cutting tool behaved correctly despite the cutting force is increased x1.33 and cutting torque is increased x1.5-2, with respect to Ti4Al6V. When feed rates values are multiplied x2, torque values are multiplied x1.3 approximately. Table 5 shows again the experimental data necessary to obtain the polynomials of the cutting coefficients. A higher dispersion is seen for the cutting torque T_c as the pilot hole diameter approaches the final hole diameter (Figure 5, right).

Table 5. Experimental results for F_z [N] and T_c [Nm] in TNB alloy.

	F_z [N]		T_c [Nm]	
D_0 [mm]	f [mm/rev]		f [mm/rev]	
	0.05	0.1	0.05	0.1
3	802	954	5.8	7.0
4	631	765	5.3	6.7
5	476	575	4.3	6.1
6	343	421	4.0	6.0
7	240	259	3.5	5.7

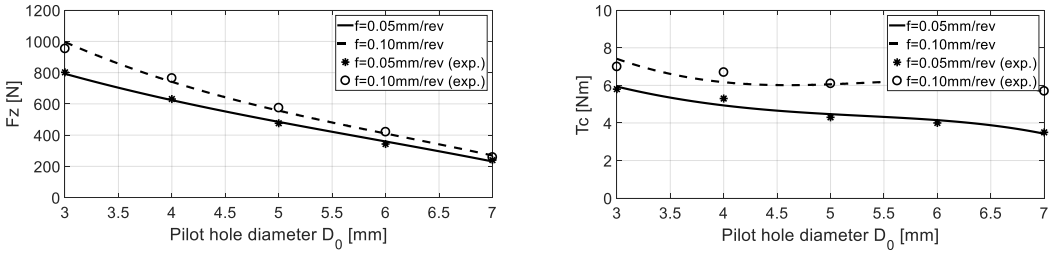

Figure 5. F_z [N] (left) and T_c [Nm] (right) for TNB alloy drilling experimental and mechanistic model values

Results for ingot MoCuSi alloy

Ingot MoCuSi alloys are harder Ti-6Al-4V alloys and TNB alloys. This statement was verified on sight of Figure 6. The axial force F_z and cutting torque T_c is higher regarding to previous alloys. Focusing on cutting torque (Figure 6 right), when the feed rate value is multiplied x2, torque values are multiplied x1.1 approximately.

Preprints (www.preprints.org) | NOT PEER-REVIEWED | Posted: 29 October 2018 doi:10.20944/preprints201810.0646.v1

Peer-reviewed version available at Materials 2018, 11, 2379; doi:10.3390/ma11122379

Table 6. Experimental results for F_z [N] and T_c [Nm] in ingot MoCuSi alloy.

D_0 [mm]	F_z [N]		T_c [Nm]	
	f [mm/rev]		f [mm/rev]	
	0.05	0.1	0.05	0.1
3	852	906	6.0	8.7
4	702	775	5.5	8.3
5	525	600	4.8	7.5
6	419	466	4.6	7.3
7	275	290	4.0	7.0

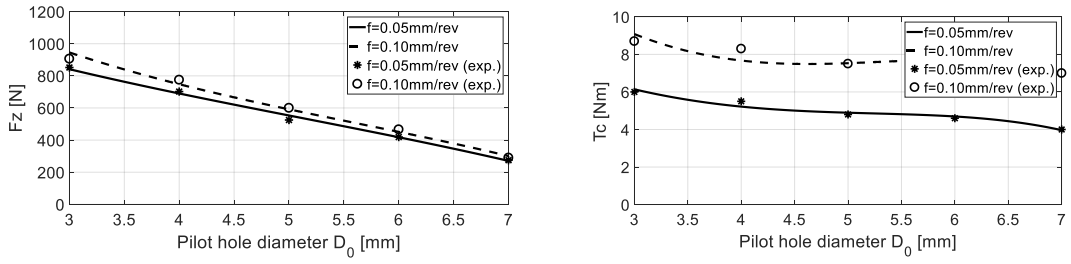

Figure 6. Fz [N] (left) and Tc [Nm] (right) for ingot MoCuSi alloy drilling experimental and mechanistic model values

Results for extruded MoCuSi alloy

MoCuSi extruded alloys presents the highest hardness values in comparison to the latter ones. While the results for the cutting torque T_c are quite similar to the ingot MoCuSi alloy (both results are almost identical), the thrust force is more dramatic to the extruded MoCuSi alloy. Regarding cutting torque (Figure 7 right), when the feed rate value is multiplied by two, torque values are multiplied x1.2 approximately.

Table 7. Experimental results for F_z [N] and T_c [Nm] in extruded MoCuSi alloy

D_0 [mm]	F_z [N]		T_c [Nm]	
	f [mm/rev]		f [mm/rev]	
	0.05	0.1	0.05	0.1
3	925	1050	6.5	9.3
4	751	860	6.1	8.6
5	550	621	5.5	8.0
6	427	475	4.7	7.7
7	280	292	4.0	7.5

Preprints (www.preprints.org) | NOT PEER-REVIEWED | Posted: 29 October 2018 doi:10.20944/preprints201810.0646.v1

Peer-reviewed version available at Materials 2018, 11, 2379; doi:10.3390/ma11122379

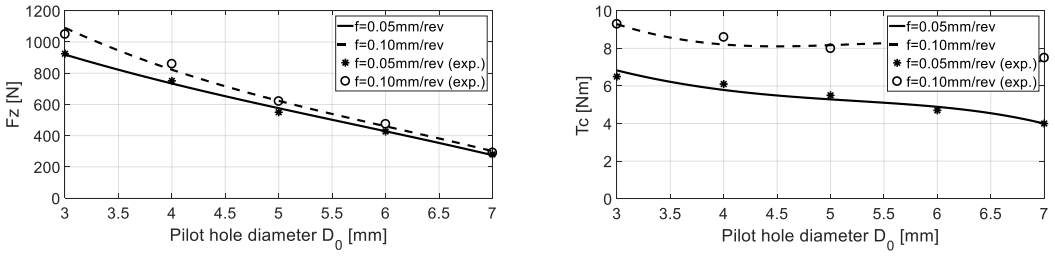

Figure 7. Fz [N] (left) and Tc [Nm] (right) for extruded MoCuSi alloy drilling experimental and mechanistic model values.

Using the above experimental results, the coefficients in Eqs.3-4 are obtained and so, the corresponding polynomial functions are built (Table 8).

Table 8. Obtained coefficients for the polynomials in Eqs. (3-4).

Materials	$K_z(h,r)$	$K_T(h,r)$
Ti-6Al-4V	a_0= 13,159; a_1= -93,861; a_2= -3,225; a_3= -10,986; a_4= 977.11; a_5= -7,056.0	b_0= 39.646; b_1= -68.280; b_2= -21.597; b_3= -41.882; b_4= 5.253; b_5= -5.171
TNB	a_0= 19,860; a_1= -217,630; a_2= -3,830; a_3= 17,235; a_4= 855.42; a_5= -16,347.1	b_0= 77.853; b_1= -283.109; b_2= -36.204; b_3= -61.168; b_4= 8.334; b_5= -21.331
MoCuSi (ingot)	a_0= 23,445; a_1= -270,543; a_2= -4,028; a_3= 20,962; a_4= 688.07; a_5= -20,320	b_0= 90.152; b_1= -274.538; b_2= -45.120; b_3= -17.808; b_4= 9.663; b_5= -20.703
MoCuSi (extruded)	a_0= 24,016; a_1= -282,289; a_2= -4,270; a_3= 24,114; a_4= 860.73; a_5= -21,202	b_0= 84.201; b_1= -120.895; b_2= -45.120; b_3= -17.808; b_4= 9.663; b_5= -20.703

For model validation, different combinations of parameters were tested within the window parameters. New pilot hole drills and final drill of D = 8.5 mm were used for these tests. 8 different tests were programmed to put the model to work. Table 9 presents the conditions for these validation tests.

Table 9. Cutting conditions for the validation tests

Materials	V_c [m/min]	D_0 [m/min]	f [mm/rev]	# *Test*
Ti-6Al-4V	50	4	0.06	1
		6	0.08	2
TNB	15	4	0.06	3
		6	0.08	4
MoCuSi (ingot)	15	4	0.06	5
		6	0.08	6
MoCuSi (extruded)	15	4	0.06	7
		6	0.08	8

Figure 8 shows the results from the simulated values using the model described and the experimentally measured values. The model presents a good correlation with the real thrust forces and cutting torques. For the cutting forces the maximum relative error between the predicted and measured values was 8% while for the cutting torque the worst case was found at 13%.

Preprints (www.preprints.org) | NOT PEER-REVIEWED | Posted: 29 October 2018 doi:10.20944/preprints201810.0646.v1

Peer-reviewed version available at Materials 2018, 11, 2379; doi:10.3390/ma11122379

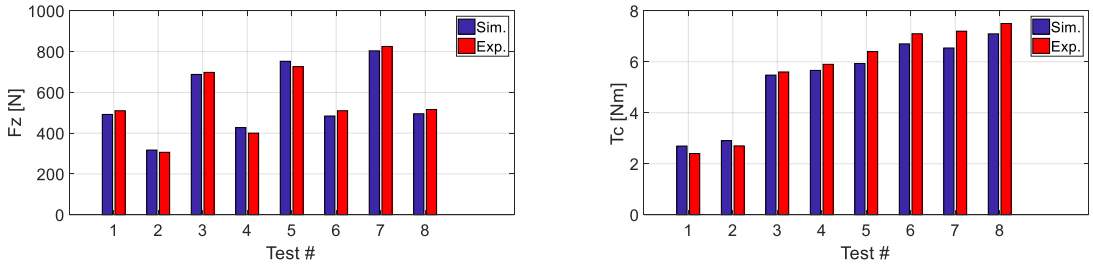

Figure 8. Model validation for F_z and T_c magnitudes.

6. Conclusions

This work presents the machinability results for 4 different titanium alloys. Currently there are few data about machining of γ-TiAl. The obtained results reflect that these alloys present a much smaller machinability than conventional titanium alloys. Three manufactured presentations for these alloys are in the market, the TNB alloy, the alloy solidified as ingot, and the alloy extruded after solidification. These are very brittle materials, so a special care must be paid to avoid the chipping and cracking of components during machining processes [35-36]. Besides, two serious disadvantages during their processing are their great sensibility to the impurity during the foundry process and so, high production costs.

This work presents a mechanistic stationary model capable of simulating the thrust force and cutting torque in the drilling process. The influence of vibratory effects, lateral vibrations or runout was not considered. After model calibration, validation tests were done showing a good agreement.

Experimental drilling tests were done to evaluate the machinability of these difficult-to-cut materials. The high cost of the tested materials (approx. 400 €/kg) limited the number of tests and a stronger experimental design. In sight of the obtained cutting coefficients, a quasi-linear dependence on the pilot hole D_0 was found for the axial force F_z while a cubic is more suitable in the case of T_c.

The experiments demonstrated big differences between the more conventional Ti6Al4V alloy and the three γ-TiAl intermetallic alloys. As the mechanical properties of extruded/ingot alloys are higher than the TNB alloy, this trend is inversely true for the machinability grade. Tests proved that MoCuSi alloys are the toughest materials.

Despite the good results during the validation, a statistical approach would be desirable to test any differences in material series, machine tools, etc. as well as to build more complete models. Wear studies including process damping effects can be subjects for future research works.

Author Contributions: A.B. designed and performed the experiments. G.U. and A.C. analyzed obtained experimental and mechanistic model predicted results. Finally, L.N.L.d.L. contributed with the resources (machine, tools, material, etc.) and general supervision of the work.

Funding: Acknowledgments: Thanks are addressed to the UFI in Mechanical Engineering of the UPV/EHU for its support to this project, and to Spanish project DPI2016-74845-R, ESTRATEGIAS AVANZADAS DE DEFINICION DE FRESADO EN PIEZAS ROTATIVAS INTEGRALES, CON ASEGURAMIENTO DE REQUISITO DE FIABILIDAD Y PRODUCTIVIDAD and project RTC-2014-1861-4, INNPACTO DESAFIO II.

Acknowledgments: The authors acknowledge the technical assistance from Eng. Garikoitz Goikoetxea at UPV/EHU.

Conflicts of Interest: The authors declare no conflict of interest. The funders had no role in the design of the study; in the collection, analyses, or interpretation of data; in the writing of the manuscript, or in the decision to publish the results.

References

1. www.boeing.com

2. Martin, R.; Evans, D. Reducing Costs in Aircraft: The Metals Affordability Initiative Consortium. *JOM* **2000**, *52* (3), 24-28.
3. Voice W.E.; Henderson M.; Shelton E.F.J.; Wu, X. Gamma titanium aluminide-TNB. *Intermetallics* **2005**, *13*, 959-964.
4. Boyer, R.R. An overview on the use of titanium in the aerospace industry. *Mater. Sci. Eng. A* **1996**, *213*, 103–114.
5. Jha, A.K.; Singh, S.K.; Kiranmayee, M.S.; Sreekumar, K.; Sinha, P.P. Failure analysis of titanium alloy (Ti6Al4V) fastener used in aerospace application. *Eng. Fail. Anal.* **2010**, *17*, 1457–1465.
6. Murr, L.E.; Quinones, S.A.; Gaytan, S.M.; López, M.I.; Rodela, A; Martinez, E.Y.; Hernandez, D.H.; Martinez, E.; Medina, F., Wicker, R.B. Microstructure and mechanical behavior of Ti-6Al-4 V produced by rapid-layer manufacturing for biomedical applications. *J. Mech. Behav. Biomed. Mater.* **2009**, *2*, 20–32.
7. Yamaguchi, M.; Inui, H.; Ito, K. High temperature structural intermetallics. *Acta Mater* **2000**, *48*, 307-322.
8. Kim Y.W.; Dimiduk, D.M. Gamma TiAl alloys: emerging new structural metallic materials. Proceeding of ICETS 2000-ISAM, 2000, Beijing.
9. Semiatin S.L.; Seetharaman, V., Weiss, I. Hot workability of titanium and titanium aluminide alloys. *Mater Sci Eng.* **1998**, *243*, 1-24.
10. López de Lacalle, L.N.; Perez, J.; Llorente, J.I.; Sanchez, J.A. Advanced cutting conditions for the milling of aeronautical alloys. *J. Mater. Process. Technol.* **2000**, *100*, 1–11.
11. Aspinwall D.K.; Dewes, R.C.; Mantle, A.L. The Machining of g-TiAl Intermetallic Alloys. *CIRP Ann. - Manuf. Tech.* **2005**, *54(1)*, 99–104.
12. Arrazola, P.J.; Garay, A.; Iriarte, L.M.; Armendia, M.; Marya, S.; Maitre, F.L. Machinability of titanium alloys (Ti6Al4V and Ti555.3). *J. Mater. Process. Technol.* **2009**, 209, 2223–2230.
13. Beranoagirre, A.; López de Lacalle, L.N. Grinding of Gamma TiAl Intermetallic Alloys. *Proc. Eng.* **2013**, *63*, 489-498.
14. Lindemann, J.; Glavatskikh, M.; Leyens, C. Surface effects on the mechanical properties of gamma titanium aluminides. 7th THERMEC, 2011, Canada.
15. Hood, T.; Aspinwall, D.K.; Sage, C.; Voice, W. High speed ball nose and milling of γ-TiAl alloys. *Intermetallics* **2013**, *32*, 284-291.
16. Thepsonthi, T.; Ozel, T. Experimental and Finite Element Simulation based Investigations on Micro-Milling Ti–6Al–4V Titanium Alloy: Effects of cBN Coating on Tool Wear. *J. Mater. Process. Technol.* **2013**, *213*, 532–542.
17. Cantero, J.L.; Tardio, M.M.; Canteli, J.A.; Marcos, M.; Miguelez, M.H. Dry drilling of alloy Ti6Al4V. *Int. J. Mach. Tools Manuf.* **2005**, *45*, 1246–1255.
18. Hood, R.; Aspinwall, D.K.; Soo, S.L.; Mantle, A.L.; Novovic, D. Workpiece surface integrity when slot milling γ-TiAl intermetallic alloy. *CIRP Ann.* **2014**, *63(1)*, 53-56.
19. Liu, J.; Zhu, D.; Zhao, L.; Xu, Z. Experimental Investigation on Electrochemical Machining of γ-TiAl Intermetallic. *Proc. CIRP* **2015**, *35*, 20-24.
20. Kosaraju, S.; Anne, V.G. Optimal machining conditions for turning Ti-6Al-4 V using response surface methodology, *Adv. Manuf. Technol.* **2013**, *1(4)*, 329–339.
21. Mantle, A.L.; Aspinwall, D.K. Temperature Measurement and Tool Wear When turning gamma titanium aluminide intermetallic, Proceedings of the 13th Conference of the Irish manufacturing Committee (IMC-13). Re-Engineering for World Class manufacturing, Limerick, Ireland, (1996), 427-446.
22. Aspinwall, D.K.; Mantle, A.L.; Chan, W.K.; Hood, R.; Soo S.L. Cutting Temperatures when Ball Nose End Milling g-TiAl Intermetallic Alloys. *CIRP Ann.* **2013**, *62(1)*, 75–78.
23. Mantle, A.L.; Aspinwall D.K. Surface integrity of a high speed milled gamma titanium aluminide. *J. Mater. Process. Technol.* **2001**, 118, 143-150.
24. Olvera, D.; Urbicain, G.; Beranoagirre, A. López de Lacalle, L.N. Hole Making in Gamma TiAl. DAAAM International scientific book, 337-347, 2010.

25. Priarone, P.C.; Rizzuti, S.; Settineri, L.; Vergnano, G. Effects of Cutting Angle, Edge Preparation and Nano-Structured Coating on Milling Performance of a Gamma Titanium Aluminide. *J. Mater. Process. Technol.* **2012**, *212*, 2619–2628.
26. Hong, S.Y.; Ding, Y. Cooling approaches and cutting temperatures in cryogenic machining of Ti-6Al-4 V. *Int. J. Mach. Tools Manuf.* **2001**, *41*, 1417–1437.
27. Marasi, A. Modeling the effects of cutting parameters on the main cutting force of Ti6Al4V alloy by using hybrid approach. *Int. J. Adv. Eng. Appl*. **2013**, *2(5)*, 6–14.
28. Kadirgama, K.; Abou-El-Hossein, K.A.; Mohammad, B.; Habeeb, A.; Noor, M.M. Cutting force prediction model by FEA and RSM when machining Hastelloy C-22HS with 90 °holder. *J. Sci. Ind. Res.* **2008**, *67*, 421–427.
29. Bagci, E.; Ozcelik, B. Finite element and experimental investigation of temperature changes on a twist drill in sequential dry drilling. *Int. J. Adv. Manuf. Technol.* **2006**, *28*, 680–687.
30. Chatterjee, S.; Mahapatra, S.S.; Abhishek, K. Simulation and optimization of machining parameters in drilling of titanium alloys. *Sim. Mod. Prac. Th.* **2016**, *62*, 31-48.
31. Azeem, A.; Feng H.Y.; Wang, L. Simplified and efficient calibration of a mechanistic cutting force model for ball-end milling. *Int. J. Mach. Tools Manuf.* **2004**, 44, 291–298.
32. Altintas, Y. (2000) Manufacturing automation. Cambridge University press.
33. Budak, E.; Altintas, Y.; Armarego, E.J.A. Prediction of milling force coefficients from orthogonal cutting data. ASME J. Manuf. Sci. Eng. **1996**, *118(2)*, 216-224
34. Roukema, J.C.; Altintas, Y. Time domain simulation of torsional–axial vibrations in drilling. *Int. J. Mach. Tools Manuf.* **2006**, *46(15)*, 2073-2085.
35. Beranoagirre, A.; Olvera, D.; López de Lacalle, L.N.; Urbicain, G. Drilling of intermetallic alloys gamma TiAl, AIP Conference Proceedings *1315 (1)*, 1023-1028.
36. Beranoagirre, A.; Urbicain, G.; Calleja, A.; López de Lacalle, L.N. Hole Making by Electrical Discharge Machining (EDM) of γ-TiAl Intermetallic Alloys. *Metals* **2018**, *8*(7), 543.